Research Article

3D QSAR and In Silico Docking Studies of Natural Flavonoid Derivatives as Acetylcholinesterase Inhibitors

Shravan Kumar Gunda*, Suchitra pasula, Venu Gurram, Mahmood Shaik
Bioinformatics Division, Osmania University, Hyderabad, India.
*Corresponding author's E-mail: gunda14@gmail.com

ABSTRACT

Comparative molecular field analysis (CoMFA) and comparative molecular similarity indices analysis (CoMSIA), three-dimensional quantitative structure activity relationship (3D-QSAR) techniques, were applied to a set of 53 natural flavonoids as Acetylcholinesterase inhibitors (training set 46 molecules, test set 7 molecules). The best CoMFA model yielded the cross-validated q^2 - 0.810 and the non-cross-validated r^2 - 0.961. The derived model indicated the importance of steric (63.2%) as well as electrostatic (36.8%) contributions. For CoMSIA studies, different combinations of the fields were tested. The best CoMSIA model gave q^2 - 0.583 and r^2 - 0.947. This model showed that steric (20.7%), electrostatic (23.0%), hydrophobic (21.3%) hydrogen bond donor (20.0%) and hydrogen bond acceptor (15.0%) properties played major role in Alzheimer's. FlexX were employed to dock the inhibitors into the active site of the acetyl-cholinesterase enzyme and these docking studies revealed the vital interactions and binding conformation of the inhibitors.

Keywords: 3D-QSAR; CoMFA; CoMSIA; Natural Flavonoids; Acetylcholinesterase; Alzheimer's; FlexX Docking

INTRODUCTION

Acetylcholinesterase (EC 3.1.1.7, AChE) is one of the most essential enzymes in the family of serine hydrolases, which catalyzes the hydrolysis of neurotransmitter acetylcholine, which is important class of medicinal agents useful for the treatment of Alzheimer's disease, myasthenia gravis, glaucoma and for the recovery of neuromuscular block in surgery[1]. Acetylcholinesterase is a target enzyme for biologically active compounds including anti-Alzheimer's disease agents. Alzheimer's disease is a progressive neuro-degenerative disorder of the central nervous system, is the most common cause of dementia amongst elderly people[2]. AChE plays a key role in loss of memory and cognition. Patients with Alzheimer's disease exhibit a significant decrease in cognitive ability and severe behavioral and psychological abnormalities such as anxiety, irritability and depression[3].

The main function of the AChE is hydrolytic destruction of the neurotransmitter acetylcholine, which terminates in impulse transmission at cholinergic synapses. Acetylcholine exerts many physiological functions both in the central nervous system and periphery[4,5] for example modulation of cardiac rate, motor control, smooth muscle contraction, force, pain modulation, temperature regulation and memory etc.

Acetylcholinesterase is bound to the basement membrane in the synaptic cleft at cholinergic synapses. It is also present in cholinergic nerve terminals, where it seems to have an important role in regulating the free acetylcholine concentration and from it may be secreted[6]. Synaptic junctional and extra junctional are the two different classes of quaternary structures of acetylcholinesterase, which are distinguishable by their solubility and hydrodynamic properties.

Flavonoids are a group of poly-phenolic compounds, different in their chemical structure and characteristics and are found universally in plants. Chemically they are C6-C3-C6 compounds in which two C6 groups are substituted benzene rings, and the C3 position is an aliphatic chain which contains a pyran ring[7]. There are more than 9000 different flavonoid compounds derived from plants and are sub-grouped into flavonols, flavanones, flavones, chalcones, anthocyanins, flavanidiols, pro-anthocyanidins etc.[8]. They play significant biological roles by affecting several developmental processes[9]. Flavonoids are commonly found predominantly in almost all plant parts which include seeds, flowers, fruit, stems, leaves, roots, vegetables etc., hence they form one of the constituents in human diet[10]. In recent times flavonoid class of natural products are increasingly used as subjects for anti-proliferative research, and many groups of flavonoids were observed to have anti-Alzheimer, anti-oxidant, anti-bacterial, anti-inflammatory, anti-infective, anti-cancer, anti-viral and antifungal activity[11].

In the present study 53 natural flavonoid derivatives as Acetylcholinesterase inhibitors were performed using three dimensional quantitative structure activity relationships and insilico docking approach. Three dimensional quantitative structure activity relationship (3D-QSAR) methods, such as CoMFA (Comparative molecular field analysis)[12] and CoMSIA (Comparative molecular similarity indices analysis)[13] were applied to these inhibitors to gain insights into how steric, electrostatic, hydrophobic; hydrogen bonding interactions influence their activities. Docking study was

performed to explore the binding mode between all of the compounds and the Acetylcholinesterase, which produced the bioactive conformer of the whole dataset. Based on the molecular field information of 3D-QSAR tools and molecular docking protocols, a few strategies were proposed to design new molecules with improved activity.

MATERIALS AND METHODS

Molecular Structures and Optimization

A series of fifty three natural flavonoid molecules selected for the present study were taken from an earlier report[14-28]. The compound names and their biological activities are given in **Table 1**. *In vitro* AChE inhibitory activities were converted into the corresponding pIC50 (-log IC50) values. These experimental activities are used as dependent variables in Comparative molecular field analysis (CoMFA) and Molecular similarity indices analysis (CoMSIA).

The total set of AChE inhibitors (53 compounds) was randomly divided into training set (46 compounds) and test set (7 molecules).

All the 3D structures of Flavonoid derivatives were sketched by using Sybyl program package version 6.7[29] on a silicon graphic workstation. Present study, each structure of 53 compounds was first minimized using Tripo's force field with a 0.005 kcal/mol Å energy gradient convergence criterion.

Charges were calculated by the Tripo's method at the beginning and Gasteiger-Huckel was considered for the further calculations.

Molecular Alignment

Molecular alignment is the most sensitive parameter in three dimensional quantitative structure activity relationship studies. The quality and predictive power of the model were directly dependent on the alignment rule[30]. CoMFA results are not sensitive to a number of factors such as alignment, lattice shifting step size and probe atom type. Structural alignment play important role in prediction of CoMFA models and the reliability of the contour models depend strongly on the structural alignment of the molecules. The molecular alignment was achieved by SYBYL routine align database module.

The most active compound Kurarinone was used as a template to align the other 52 compounds from the series by common substructure alignment, using the align database command in SYBYL 6.7.

The template molecule is typically most active, lead molecule and the compound contains more number of functional groups.

Basic skeleton of the flavonone is shown in Fig 1(a), and the superimposed structure after alignment is presented in Fig 1(b).

CoMFA Studies

Steric and electrostatic fields are calculated using the Lennard-Jones and Coulomb potentials with a distance-dependent dielectric constant at all interactions in a regularly spaced (2Å) grid taking a sp^3 carbon atom as steric probe and a+1 charge as electrostatic probe. The cutoff value was set to 30kcal/mol, it indicates the electrostatic and steric energies >30 kcal/mol are truncated to that value, thus, can avoid infinity of energy values inside molecule[31]. With standard options for scaling of variables, regression analysis was carried out using the fully cross-validated partial least squares (PLS) method (leave one out). Optimum number of components (N=5) used in the model derivation. The column filtering was set 2.0 kcal/mol to get better the signal to noise ratio by omitting those lattice points whose energy variation was below this threshold.

The cross-validated coefficient q^2 was calculated according to the following equation:

$$q^2 = 1 - \frac{\sum \left(Y_{pred} - Y_{actu} \right)^2}{\sum \left(Y_{actu} - Y_{mean} \right)^2}$$

Where Y_{pred}, Y_{actu} and Y_{mean} are predicted, actual and mean values of the target property (pIC50), respectively; and

$$\sum \left(Y_{actu} - Y_{mean} \right)^2 = PRESS$$

PRESS is the prediction error sum of the squares, derived from the LOO method. The ONC (Optimum number of components) corresponding to the lowest PRESS value was used for deriving the final Partial least square regression models. By using the same number of components performed the Non-cross-validation to calculate conventional r^2.
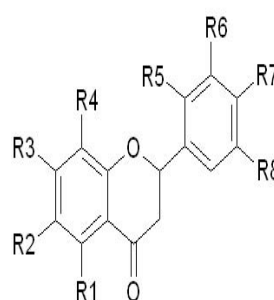

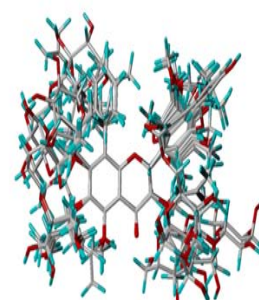Fig.1(a) Basic skeleton of flavonone

Fig.1(b). 3D-view of aligned molecules (training set and test set) based on SYBYL routine database align method

The q^2 quantifies the predictive ability of the model. It was determined by LOO procedure of cross validation in which each molecule is successively removed from the model derivation and its pIC50 value can be predicted using the model build from the remaining molecules. The CoMFA model is calculated by two statistical parameters: q^2 and r^2. q^2 indicates predictive capability of the model, should be >0.5. The value r^2 indicates self-consistency of the model, it should be >0.9.

Table 1: Compounds used in training set and test set. Bold indicates test set. Experimental and predicted values with dock score.

Compound number	pIC50	CoMFA		CoMSIA		Dock Score
		Predicted	Residual	Predicted	Residual	
5-geranyl-5,7,2α,4α-tetrahydroxyflavone	6.284	6.277	0.007	5.836	0.448	-19.6
5-hydroxy-7,4α-dimethoxyflavone	4.027	4.563	-0.536	4.916	-0.889	-23.1
Irigenin-7-O-β-D-glucopyranoside	**7.155**	**6.193**	**0.962**	**6.393**	**0.762**	**-21.1**
Irilone	7.155	6.959	0.196	6.939	0.216	-18.4
Irisolone-4'-O-β-D-glucopyranoside	7.155	6.810	0.345	6.354	0.801	-12.3
Iso-Osajin	5.870	6.146	-0.276	6.103	-0.233	-14.7
Iso-pomiferin	**5.573**	**6.237**	**-0.664**	**5.282**	**0.591**	**-22.6**
Osajiin	5.650	6.473	-0.823	6.337	-0.687	-13.8
Pomiferin	7.018	6.095	0.923	6.337	0.681	-20.7
Acacetin	6.194	5.866	0.328	5.773	0.421	-21.3
Apigenin	**6.194**	**5.920**	**0.274**	**5.956**	**0.238**	**-19.4**
Cirsimaritin	4.089	4.362	-0.273	4.430	-0.341	-17.9
Eupatilin	4.089	4.068	0.021	4.725	-0.636	-21.8
Isolinariin A	6.569	6.497	0.072	6.457	0.112	-11.0
Isolinariin B	6.569	6.666	-0.097	6.534	0.035	-13.2
Isoorientin	7.155	7.006	0.149	7.328	-0.173	-20.6
isorientin-6-O-β-D-glucopyranoside	7.155	7.323	-0.168	7.063	0.092	-21.1
Isovitexin	7.155	7.151	0.0004	6.548	0.607	-15.7
Isovitexin-6-O-β-D-glucopyranoside	7.155	7.192	-0.037	6.722	0.433	-17.9
Linariin	6.569	6.653	-0.084	6.263	0.306	-11.3
Luteolin-7-O-rutinoside	4.001	4.199	-0.198	3.023	0.978	-18.0
Cyclomorusin	6.284	6.087	0.197	5.927	0.357	-14.4
Kuwanon C	6.284	7.073	-0.789	6.515	-0.231	-17.0
Morusin	6.284	5.965	0.319	5.545	0.739	-18.0
Morusinol	6.284	6.088	0.196	5.969	0.315	-20.8
Neocyclomorusin	6.284	6.171	0.113	6.613	-0.329	-14.8
(2S)-5,2α-dihydroxy-7,5-dimethoxyflavone	4.492	4.856	-0.364	4.789	-0.297	-19.5
Hispidone	4.492	4.824	-0.332	5.134	-0.642	-22.6
Kurarinone	7.824	7.222	0.602	6.991	0.833	-11.0
Kuwanon E	6.284	5.529	0.755	6.089	0.195	-21.3
Kurarinol	7.824	7.308	0.516	7.045	-0.779	-15.6
3,5,7,3α,4α-pentamethoxyflavone	4.027	4.222	-0.395	4.518	-0.491	-23.7
3,5,7,4α-tetramethoxyflavone	4.207	4.995	-0.968	4.324	-0.297	-19.7
3-methoxyquercetin	**4.423**	**5.390**	**-0.967**	**5.021**	**-0.598**	**-28.3**
5,7,4'-trihydroxy-3,3'-dimethoxyflavone	6.180	5.581	0.599	5.579	0.601	-26.9
8-C-Lavandulylkaempferol	6.886	7.759	-0.693	7.125	-0.239	-21.5
5,7,4α-trimethoxyflavone	4.027	4.540	-0.513	4.926	-0.899	-23.2
Acaciin	6.194	6.275	-0.081	6.267	-0.073	-21.7
Ayanin-(5,3α-dihydroxy-3,7,4α-trimethoxyflavone	4.027	4.354	-0.327	4.356	-0.329	-23.1
Desmethylandydroicaritin	6.886	6.542	0.344	6.433	0.453	-18.7
Galangin	**4.035**	**4.080**	**-0.045**	**3.251**	**0.084**	**-19.6**
Gossyptein-7-O-l-rhamnopyranoside	4.001	4.852	-0.851	4.324	-0.323	-21.8
5,7-dimethoxyflavone	4.027	4.916	-0.889	5.009	-0.982	-16.4
Icaritin	6.886	6.115	0.771	6.615	0.271	-21.8
Kaempferol-3-O-β-D-glucopyranoside	7.155	6.834	0.321	6.958	0.197	-14.6
Kushenol C	7.824	6.973	0.851	6.999	0.825	-16.6
Myricetin-3',5'-dimethylether-3-O-β-D-galactopyranoside	7.000	6.517	0.483	6.501	0.499	-15.3
Myricetin-3'-methylether-3-O-β-D-galactopyranoside	7.000	7.389	-0.389	7.092	-0.092	-18.9
Quercetin	**4.423**	**5.011**	**-0.588**	**4.491**	**-0.068**	**-22.5**
5α-geranyl-4α-methoxy-5,7,2α-trihydroxyflavone	6.284	6.345	-0.061	5.518	0.766	-17.5
Rhodioflavonoside	4.001	3.956	0.405	4.587	-0.586	-8.80
Sophoflavescenol	6.886	6.459	0.427	6.310	0.576	-20.8
Tiliroside	**4.423**	**5.160**	**-0.737**	**4.992**	**-0.569**	**-13.6**

CoMSIA Studies

CoMSIA approach is a substitution to perform 3D-QSAR by CoMFA. Molecular similarity is compared in terms of similarity indices. In Comparative Molecular Similarity Indices Analysis, a distance-dependent Gaussian-type physicochemical function has been adopted to avoid uniqueness at the atomic positions and dramatic changes of potential energy for those grids in the proximity of the surface[32]. The CoMSIA method specifies explicit steric, electrostatic along with hydrophobic, hydrogen bond donor and acceptor fields, were calculated using the sp^3 carbon probe atom with a +1 charge atom and a radius of 1.0 A°. In CoMFA Steric and electrostatic fields were calculated. Primarily, the intention is to division the different properties into various placements where they play a decisive role in determining the biological activity. In general, molecular similarity indices, i.e., $A_{F,K}$ between the compounds of interest were computed by placing a probe atom at the intersections of the lattice points using below equation:

$$A_{F,K}^{q}(j) = \left|-\sum_{i=1}^{n} W_{probe,k} W_{ik} e^{-a r_{iq}^2}\right.$$

where q is a grid point, i is a summation index over all atoms of the molecule j under computation, W_{ik} is actual value of the physicochemical property k of atom i, and $W_{probe,k}$ is value of the probe atom.

In the present study, similarity indices were computed using a probe atom ($W_{probe,k}$) with charge +1, radius 1Å, hydrophobicity +1, and attenuation factor a of 0.3 for the Gaussian type distance. The statistical valuation for the CoMSIA analyses was performed in the same manner as described for CoMFA.

RESULTS AND DISCUSSION

3D QSAR Studies

CoMFA and CoMSIA 3D-QSAR models were derived using Acetylcholinesterase inhibitors. Molecule name, their experimental pIC50, predicted, residual and dock score values are given in Table 1.

CoMFA Analysis

Forty six compounds out of the total fifty three cholinesterase inhibitors were used as training set and seven compounds were used as test set. The test set compounds were selected randomly so that the structural diversity and wide range of activity in the dataset were considered included. Partial least square analysis was carried out for the training set and a cross-validated q^2 of 0.810 for five components. The non cross-validated PLS analysis with the optimum components revealed a conventional r^2 value of 0.961, F value = 196.689 and an estimated standard error of estimate (SEE) 0.270. The steric field descriptors contribution is 63.2 % of the variance, while the electrostatic field contribution is 36.8 % of the variance. 100 runs were carried out for

Bootstrap analysis for further validation of the model by statistical sampling of the original dataset to create new datasets. Correlation between CoMFA and CoMSIA experimental vs predicted were shown in Fig 2 (a) and 2 (b) respectively. The statistical analysis is given in Table 2.

CoMSIA Analysis

The CoMSIA analyses were performed using five descriptor fields: steric, electrostatic, hydrophobic, hydrogen bond donor and acceptor. The CoMSIA study disclosed a cross validated q^2 of 0.583 with optimum number of component 6, a conventional r^2 of 0.947 with a standard error of estimate 0.111 and F value 243.934. The steric field contribution 20.7 % of the variance and, the electrostatic descriptor explains 23.0 %, the hydrophobic field explains 21.3% while the hydrogen bond donor explains 15.0 % of the variance and hydrogen bond acceptor field contribution is 20.0%. For Bootstrap 100 runs was then carried out for model validation by statistical sampling of the original dataset to create new datasets. This yielded higher r^2 bootstrap value 0.990 for CoMSIA with standard error of estimate 0.318 affirming the statistical validity of the developed models.

Table 2: Statistical analysis of CoMFA and CoMSIA

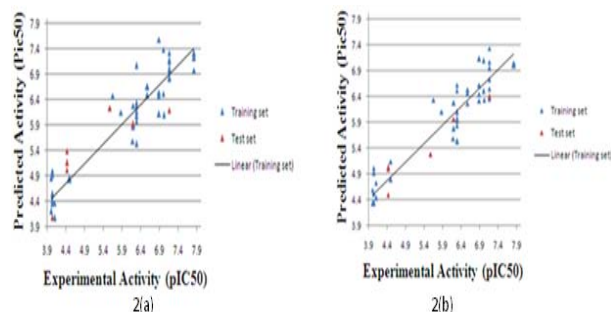| Field Name	CoMFA		CoMSIA	
q^2	0.810		0.583	
r^2	0.961		0.941	
Standard Error of Estimate	0.270		0.318	
F value	196.689		116.413	
Cross Validation				
Bootstrap	Mean	Std.dev	Mean	Std.dev
	0.197	0.129	0.224	0.150
	0.977	0.011	0.972	0.013
Field Contributions (%)				
Steric	63.2		20.7	
Electrostatic	36.8		23.0	
Hydrophobic	-		21.3	
Donor	-		20.0	
Acceptor	-		15.0	

Figure 2(a): Predicted and observed activities of training and test sets using (a) CoMFA and (b) CoMSIA models

Molecular Docking

Molecular docking studies were performed using flexX software, installed on Silicon Graphics Inc octane2

workstation using the package SYBYL6.7, to investigate the binding mode between the inhibitors and AChE. FlexX[33] is a fragment based method. FlexX handles the flexibility of the ligand by decomposing the ligand into fragments and performs the incremental construction algorithm directly inside the protein active site. This method allows conformational flexibility of the ligand while keeping the protein rigid. The base fragment is selected such that it has most potential interaction groups and the fewest alternative conformations. All the 53 molecules which were used in QSAR studies are taken for molecular docking studies. The crystal structure of AChE (PDB ID: 1EVE) in the complex with NAG (N-acetyl-D-Glucosamine) was used in the study. While creating RDF file, active site was defined within a radius 6.5Å of the ligand. Formal charges were assigned to all the molecules and the molecules were docked. FlexX generated 30 different conformations in the active site. All these conformations are ranked according to the FlexX score.

Contour Analysis

CoMFA steric field defined by the green colored (80% contribution) contours represent regions of high steric tolerance and yellow color (20% contribution) contours represent regions of unfavorable steric effect. The blue colored (80% contribution) contours represent the regions where positively charged groups enhanced the activity. Red colored (20% contribution) contours where negative charged groups enhance the activity. Steric and Electrostatic contour maps are shown in Fig 4. CoMFA models explain the variations between molecules having differences in steric and electrostatic interactions. Fig 4(a) shows the steric contour map for the CoMFA models with the highly active Kurarinone (pIC50=7.82) as a reference. The steric interaction is represented by green and yellow contours. Green contours indicate the favorable, where as yellow contours indicate unfavorable for biological activity.

CoMFA Contour Analysis

In the CoMFA contour map, two green contours and two yellow contours present. A large green contour present around the side chain at R4 position and a medium sized contour was found nearer to R8 position, which indicates that a bulky substituent's were preferred in this region. Lavandulyl group is present at side chain of R4 position of a most active compound Kurarinone shown in Fig 3(a). A green contour appears which means that sterically favored substituent's will improve the biological activities of AChE inhibitors. Green contour regions indicate favorable for steric, while yellow contours indicate unfavorable for biological activity. So addition of a bulky group at this position is favorable to the inhibitory concentration. A large yellow contour appears at OH group of the R7 position and a medium sized contour present at OH group of the R3 position. It suggests that these two positions are unfavorable. A small yellow contour located at R1 position, it suggests that small

bulky groups are required to increase the biological activity.

The electrostatic contour map of CoMFA displayed in Fig 3(b). Blue color contours indicates positively charged groups which increase biological activity and also electron deficient for high binding affinity. Most active compound Kurarinone shows large contour at side chain of R4 position of lavandulyl group and a medium sized contour present nearby C=O group. It indicating that these areas contains more positively charged substituent's at these areas. Areas where negatively charged groups enhance biological activity are contoured by red contours. Seven red color contours were present around the molecule. Two large contours present at R4 position of lavandulyl group which indicates more negatively charged substituent's present in these areas. A red contour present at R1 position of OCH3 group and also a red contour located at R2 position, which indicates more negative charge substituent's present at these positions.
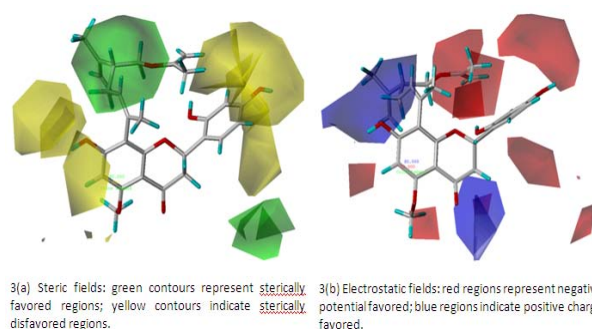

3(a) Steric fields: green contours represent sterically favored regions; yellow contours indicate sterically disfavored regions.

3(b) Electrostatic fields: red regions represent negative potential favored; blue regions indicate positive charge favored.

Figure 3: CoMFA Contour Maps

CoMSIA Contour Analysis

The CoMSIA steric contours are very similar to those of the CoMFA steric contours shown in Fig 4 (a). In CoMSIA a large green contour present at R4 position of lavandulyl group and a small green contour located nearby R8 position, which indicates that a bulky substituent's were preferred in this region. Green contours appear which means that sterically favored substituent's will improve the biological activities of AChE inhibitors. When compare to CoMFA steric green contours CoMSIA green contours are reduced in size. A large yellow contour present at R1, R2, R3 position and also another large yellow contour at R5, R6, R7, R8 position.

The electrostatic contour map of CoMSIA displayed in Fig 4(b). A large blue contour present at main ring and a small blue contour at R5 position indicating more positive charge constituents present at these positions. Most active compound Kurarinone shows large contour at side chain of R1, R2 position, two medium sized red contours are present at lavandulyl group of R4 position, and a another two medium sized contour present nearby R7, R8 groups indicating that more negative charge constituents present at these positions.

Fig 4(c) displays hydrophobic contour maps. Four white contours, a large one at the R6 position and a medium

one at the R2 position and a small one at the R3 position indicating that enhanced hydrophobic interactions disfavor the activity. Two large yellow contours present at OH group of R3 position and lavandulyl group of R4 position, which favors the increase the biological activity. Substituting hydrophilic groups in the molecule can radically increase the activity of AChE.
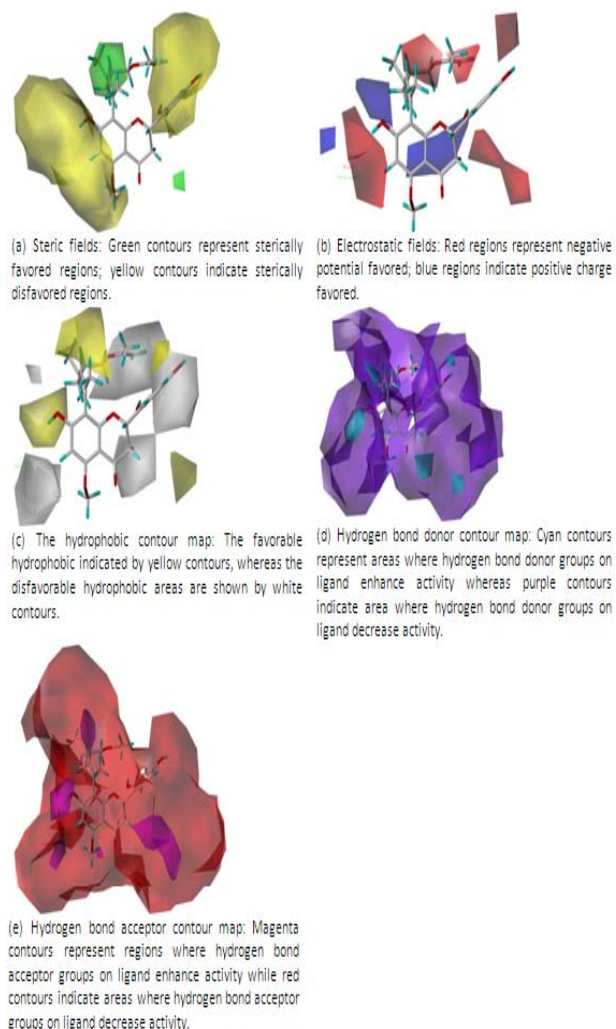

(a) Steric fields: Green contours represent sterically favored regions; yellow contours indicate sterically disfavored regions.

(b) Electrostatic fields: Red regions represent negative potential favored; blue regions indicate positive charge favored.

(c) The hydrophobic contour map: The favorable hydrophobic indicated by yellow contours, whereas the disfavorable hydrophobic areas are shown by white contours.

(d) Hydrogen bond donor contour map: Cyan contours represent areas where hydrogen bond donor groups on ligand enhance activity whereas purple contours indicate area where hydrogen bond donor groups on ligand decrease activity.

(e) Hydrogen bond acceptor contour map: Magenta contours represent regions where hydrogen bond acceptor groups on ligand enhance activity while red contours indicate areas where hydrogen bond acceptor groups on ligand decrease activity.

Figure 4: CoMSIA Contour maps

The hydrogen bond donor effect could be explained by the presence of cyan and purple colored plots; purple plots explain the favorable hydrogen bond donor fields while cyan contour plot explains the unfavorable donor fields. Total molecule is covered by cyan color indicates that hydrogen bond donor groups exhibit negative effect on the biological activity.

Three medium sized purple colored contours, one at R3 position, one at R4 position of lavandulyl group and a purple contour nearby C=O position that explains hydrogen bond donor groups exhibit positive effect on the biological activity. The hydrogen bond donor contour maps are shown in Fig 4 (d).

The CoMSIA hydrogen bond acceptor contours are represented in Fig. 4 (e) indicates areas where hydrogen-bond acceptors in the ligand promote or decrease binding affinities of the molecule.

A magenta contour in the acceptor field surrounds at R1, R2, R3, R4 and below the R8 position, indicates that substitution of hydrogen bond acceptor groups at these regions increases the inhibitory activity of the molecules against AChE. This correlation can be explained by analyzing the trends in biological data for some of the compounds. Whole molecule is covered by red contour which significantly decrease the molecule's AChE inhibitory activity.

Docking Results

Molecular docking studies have been carried out on a series of 53 natural flavonoid derivatives into the active site of acetyl cholinesterase (PDB ID: 1EVE). Analysis of the docked flavonoid compounds with the protein brought in focus some major interactions operating at the molecular level.

The binding mode of flavonoid derivatives in the binding site of human cholinesterase were identified using intermolecular flexible docking simulations by means of FlexX program. Fig 6 shows most active and least acting compounds binding conformations of the flavonoid derivatives in the binding pocket of the cholinesterase.

The most active, least active and moderate active compounds show interaction with ASP72. Most active compound Kurarinone shows interaction with Asp72, Ser286, and Phe288 with the distance between ligand and the protein is 1.94, 1.77 and 1.93 respectively. Table 3 shows interacting amino acids with their distance.

Table 3: Showing the docking interacting amino acids with their distance of most, least, moderate active compounds from the database

| Compound name	Interacting amino acid	Protein to ligand interaction	Distance (Å)
Kurarinone	Ser286	O-H12	1.771
	Phe288	H-O31	1.927
	Asp72	OD2-H9	1.939
Luteolin-7-O-rutinoside	Asp72	OD2-H7	1.198
	Asp72	OD2-H8	1.812
	Trp279	O-H18	2.120
	Asp285	OD1-H29	1.904
	Arg289	O-H10	1.609
	Arg289	H-O23	2.452
	Arg289	H-O21	2.049
	Phe288	H-O21	2.118
3-ethoxyquercetin	Asp72	OD2-H12	1.719
	Asp83	OD1-H7	2.174
	Giu199	OE1-H6	1.506
	Giu199	OE2-H6	2.135
	Ser200	HG-O22	1.703
	Ser200	OG-H11	2.637
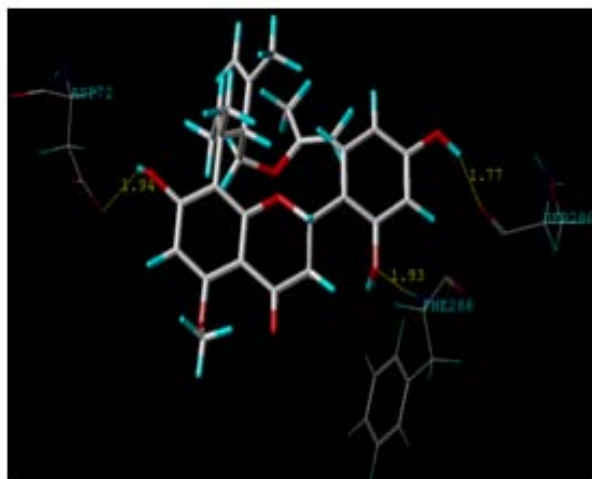
Figure 6(a): Interactions of most active compound Kurarinone with AChE. Inhibitor and the key residues within 6.5 Å around the inhibitor in AChE are represented by the capped stick and chain form, respectively. Yellow dashed lines denote the hydrogen bond distance.
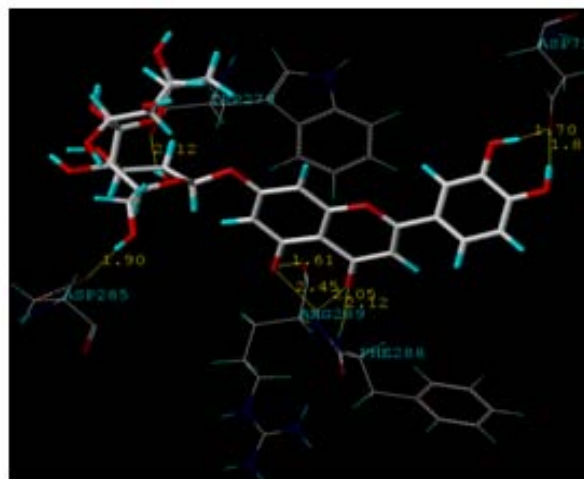

Figure 6(b): Interactions of least active compound Luteolin-7-O-rutinoside with AChE. Inhibitor and the key residues within 6.5 Å around the inhibitor in AChE are represented by the capped stick and chain form, respectively. Yellow dashed lines denote the hydrogen bond distance.

CONCLUSION

Predictive 3D-QSAR models were derived for flavonoids as inhibitors of AChE, which should be useful for assisting the design of active molecules. Such models correlate well structural features with inhibitory activities against AChE and bring valuable information about the relevant characteristics of inhibitors. The predictive ability of the models was manifested in the good correlation between actual and predicted pIC50 values for the test molecules. First, CoMFA and CoMSIA contour maps as well as docking approaches provided enough information to understand the structure–activity relationships. Reliable models were obtained by using steric and electrostatic CoMFA fields, and by using steric, hydrophobic, electrostatic, acceptor and donor for CoMSIA fields. Moreover, contour plots may help identify relevant regions where any change can affect binding preference. Furthermore, they may be helpful in identifying important features contributing to interactions between the studied flavonoids and the active site of AChE. According to the obtained statistics, prediction of AChE activities with sufficient accuracy should be possible by using these models.

REFERENCES

1. Nagaraju A, Laurent L, Janet G and Vassilios P: 3D QSAR studies of AChE inhibitors based on molecular docking scores and CoMFA. Bioorganic & medicinal chemistry letters, 16, 2006, 6277-6280.

2. Lahiri DK, Farlow MR, Greig NH and Sambamurti K: Current drug targets for Alzheimer's disease treatment. Drug Dev Res, 56, 2002, 267–281.

3. Sugimoto H, Yamanishi Y, Iimura Y and Kawakami: Donepezil Hydrochloride (E2020) and Other Acetylcholinesterase Inhibitors. Curr Med Chem, 7, 2000, 303–339.

4. Caulfield MP and Birdsall NJM: International Union of Pharmacology. XVII. Classification of muscarinic acetylcholine receptors. Pharmacol. Rev, 50, 1998, 279-290.

5. Colquhoun LM, Patrick JW: Pharmacology of neuronal nicotinic acetylcholine receptor subtypes. Adv. Pharmacol, 39, 1997, 191-220.

6. Brown SS, Kalow W, Pilz W, Whittaker M and Woronick CL: The plasma cholinesteerases: a new perspective. Adv. Clin. Chem, 22, 1981, 1-123.

7. Bylka WMI and Pilewski NA: Natural Flavonoids as Antimicrobial Agents. The Journal of the American Nutraceutical Association, 7, 2004, 24-31.

8. Williams CA and Grayer RJ: Anthocyanins and other flavonoids. Natural Product Reports, 21, 2004, 539-573.

9. Whiting DA: Natural phenolic compounds 1900-2000: a bird's eye view of a century's chemistry. Nat Prod Rep, 18, 2001, 583-606.

10. Harborne JB and Bzxter H: The handbook of natural flavonoids Volume 1 and Volume 2, Wiley, 1999.

11. Cushnie TP and Lamb AJ: Antimicrobial activity of flavonoids. Int J Antimicrob Agents, 26, 2005, 343-356.

12. Klebe G, Abraham U and Mietzner T: Molecular similarity indices in a comparative molecular field analysis (CoMFA) of drug molecules to correlate and predict their biological activity- J Med Chem, 37, 1994, 4130-4146.

13. Chakraborti AK, Gopalakrishnan B, Sobhia ME, and Malde A: 3D-QSAR studies of indole derivatives as phosphodiesterase IV inhibitors. Eur J Med Chem, 3, 2003, 975-982.

14. Bruhlmann C, Marston A, Hostesttmann K, Corrupt PA and Testa T: Screening of non-alkaloidol natural compounds as

acetyl cholinesterase inhibitors. Chem Biodivers, 1, 2004, 819-829.

15. Sawadee P, Sabphon C, Sitthiwongwanit D and Kokpol U: Anti cholinesterase activity of 7-methoxyflavones isolated from kaempferia parviflora. Phytotherapy Res, 23, 2009, 1792-1794.

16. Kim JY, Lee WS, Kim YS, Curtis-Long MJ, Lee BW, Ryu YB, Park KH: Isolation of cholinesterase–inhibiting flavonoids from Morus ihou: J Agr food Chem, 56, 2011, 4589–4596.

17. Lim SS, Han SM, Kim SY, Bae YS and Kang IJ: Isolation of acetyl cholinesterase inhibitors from the flowers of chrysanthemum indicum Linne Food Sci, Biotechnol, 16, 2007, 265-269.

18. Guo AJ, Xie HQ, Choi RC, Zheng KY, Bi CW, Xu SL, Dong TT and Tsim KW: Galangin, a flavonol derived from Rhizoma Alpiniae Officinarum, inhibits acetylcholinesterase activity *in vitro*. Chem-Biol. Interact, 187, 2010, 246-248.

19. Kolak U, Hacibekiroglu I, Oztuk M, Ozgokee F, Topeu G and Ulubelen A: Antioxidant and anti cholinesterase constituents of salvia poculata. turk J. Chem, 33, 2009, 813-823.

20. Loizzo MR, Tundis R, Menichin F, Bonesi M, Statt GA, Deguin B, Tillequin F, Menichini F and Houghton PJ: Acetyl-cholinesterase inhibition by extracts and isolated flavones from Linaria reflexa Desf. Scrophulariaceae. Nat. Prod. Commun, 2, 2007, 759-763.

21. Conforti F, Rigano D, Menichini F, Loizzo MR and Senatore F: Protection against neurodegenerative disease of Irisp seudopumila extracts and their constituents. Fitoterapia, 80, 2009, 62-67.

22. Orhan I, Senol FS, Kartal M, Dvorska M, Zemlicka M, Smejkal K and Mokry P: Cholinesterase inhibitory effects of the extracts and compounds of Maclura Pomifera (Rafin) Schaeider. Food Chem. Toxicol, 47, 2009, 1747-1751.

23. Ahmad I, Anis I, Malik A, Nawaz SA and Choudhary MI: Cholinesterase inhibitory constituents from Onusma hispida. Chem. Pharm. Bull, 51, 2003, 412-414.

24. Jung HA, Yokozawa T, Kim BW, Jung JH and Choi JS: Selective inhibition of prenylated flavonoids from sophora flavescens against BACE1 and cholinesterase. Am. J. Chinese Med, 38, 2010, 415-429.

25. Jung M and Park M: Acetyl cholinesterase inhibition by flavonoids from Agrimonia pilosa Molecules, 12, 2007, 2130-2139.

26. Jung HA, Jin SE, Park JS and Choi JS: Anti diabetic complications and Anti-Alzheimer activities of sophoflavescenol, a prenylated flavonol from sophora flavescens and its structure activity relationship. phytothera Res, 25, 2011, 709-715.

27. Hill house BJ, Ming DS, French CJ and Towers GHN: Acetyl cholinesterase inhibitions in Rhodiola rosea Pharm Biol, 42, 2004, 68-72.

28. Min BS, Cuong TD, Lee JS, Shin BS, Woo MH and Hung TM: Cholinesterase inhibitions from Cleistacalyx Operculatus Buds Arch. Pharm Res, 33, 2010, 1665-1670.

29. SYBYL6.7 is available from Tripos Associates Inc, 1699 S. Hanley Rd., St. Louis, MO 631444, USA.

30. Cramer RD, Patterson DE and Bunce JD: Comparative molecular field analysis (CoMFA) 1. Effect of shape on binding of steroids to carrier proteins. J Am Chem Soc, 110, 1988, 5959-5967.

31. Xue CX, Cui SY, Liu MC, Hu ZD and Fan BT: 3D QSAR studies on antimalarial alkoxylated and hydroxylated chalcones by CoMFA and CoMSIA European Journal of Medicinal Chemistry, 39, 2004, 745–753.

32. Klebe G, Abraham U and Mietzner T: Molecular similarity indices in a comparative analysis (CoMSIA) of drug molecules to correlate and predict their biological activity. J Med Chem. 37, 1994, 4130-4146.

33. Rarey M, Kramer B, Lengauer T and Klebe G. A fast flexible docking method using an incremental construction algorithm. J Mol Biol, 261, 1996, 470–489.

Source of Support: Nil, **Conflict of Interest:** None.